Spontaneous edge-defect formation and defect-induced conductance suppression in graphene nanoribbons

Jia Li,[1,*] Zuanyi Li,[1,†] Gang Zhou,[1] Zhirong Liu,[2] Jian Wu,[1] Bing-Lin Gu,[1] Jisoon Ihm,[3] and Wenhui Duan[1,‡]

[1]*Department of Physics, Tsinghua University, Beijing 100084, People's Republic of China*
[2]*College of Chemistry and Molecular Engineering, Peking University, Beijing 100871, People's Republic of China*
[3]*Department of Physics and Astronomy, Seoul National University, Seoul 151-747, Republic of Korea*

We present a first-principles study of the migration and recombination of edge defects (carbon adatom and/or vacancy) and their influence on electrical conductance in zigzag graphene nanoribbons (ZGNRs). It is found that at room temperature, the adatom is quite mobile while the vacancy is almost immobile along the edge of ZGNRs. The recombination of an adatom-vacancy pair leads to a pentagon-heptagon ring defect structure having a lower energy than the perfect edge, implying that such an edge defect can be formed spontaneously. This edge defect can suppresses the conductance of ZGNRs drastically, which provides some useful hints for understanding the observed semiconducting behavior of the fabricated narrow GNRs.

PACS number(s): 73.22.−f, 61.48.De, 71.15.Mb, 73.63.−b

I. INTRODUCTION

Graphene, a two-dimensional honeycomb lattice of carbon atoms, has been regarded as a new promising material for fundamental studies in condensed-matter physics since its successful synthesis in recent years.[1] Subsequently, graphene nanoribbons (GNRs), a quasi-one-dimensional structure of graphene with varying widths, were fabricated by using several methods including e-beam lithography,[2,3] chemical method,[4] metallic nanoparticle etching,[5] and microscope lithography.[6,7] As an electronic material, GNRs were found to have some excellent properties such as simple width-dependent band gaps, high carrier mobility at room temperature, and so on, which make them suitable for device applications in nanoelectronics.[2–4,8–12]

To realize practical applications of GNRs in electronics, their widths must reach true nanometer scale (≤10 nm), and consequently, edge effects become crucial.[6,13] Whereas, current GNRs fabricated in experiments inevitably have edge roughness, and their precise atomic edge structures are still unclear and need to be further determined.[4,5] Interestingly, recent experiments showed that all sub-10-nm GNRs are semiconducting[4] while previous theoretical works predicted that GNRs with perfect zigzag edges are metallic.[14] This discrepancy was suggested to originate from complicated edge structures in practice. So far, a lot of theoretical efforts were focused on the electronic structure of edge disorder by using the tight-binding method.[15] In contrast, the evolution and thermodynamics of atomic-scale edge defects have been seldom studied, especially via the first-principles approach. Therefore, exploring possible stable edge defect structures and their influence on the transport properties of GNRs is highly desired and helpful to understand recent experimental observations of GNRs and make use of GNRs in future nanoelectronics.

In this paper, with the density-functional theory (DFT) calculations, we systematically investigate the migration of typical edge defects (carbon adatom and vacancy) and the recombination of the adatom-vacancy pair (AVP) in zigzag GNRs (ZGNRs). We find that an adatom can migrate along the ribbon edge at room temperature while a vacancy cannot. The migration of carbon adatom may lead to the recombination of the AVP and the resulting pentagon-heptagon ring (R57) defect structure is more stable than the perfect edge structure. This localized R57 defect is more likely to exist at the edges of experimentally fabricated ZGNRs than periodic R57 edge structure recently proposed.[16,17] We also find that the presence of edge defects causes a decrease in the current through the ZGNR under bias voltage. Especially, for ZGNRs with the R57 edge defect, the current becomes very small and the conductance approaches zero near the Fermi level. This may play an important role in the observed semiconducting behavior of the fabricated narrow GNRs (especially those with zigzag crystallographic edges).[3,4,6]

II. METHOD AND MODEL

Our electronic-structure calculations are performed using the Vienna *ab initio* simulation package (VASP) (Ref. 18) within the framework of DFT. The projector augmented wave potential[19] and the generalized gradient approximation with Perdew-Burke-Ernzerhof functional[20] are used to describe the core electrons and the exchange-correlation energy, respectively. The cut-off energy for the plane-wave basis set is set to 400 eV. The energies are converged to below 10^{-5} eV and the residual forces on all atoms are converged to below 0.01 eV/Å. The minimum-energy path (MEP) calculations for the migration of edge defects have been performed using climbing-image nudged elastic band method.[21] The quantum transport calculations are performed using an *ab initio* code, ATOMISTIX TOOLKIT 2.0 (ATK 2.0),[22] which implements nonequilibrium Green's-function formalism with time-independent DFT.[23] This approach is limited to the steady-state regime and based on a self-consistency procedure. Such limitations make the approach different from Keldysh's nonequilibrium Green's function (see Ref. 24). Since the migration of edge defects are dominated by the atoms nearby, in the calculation of the migration path, we choose ZGNRs with the defect locating at one ribbon edge and the other edge being perfect as the models. To exclude
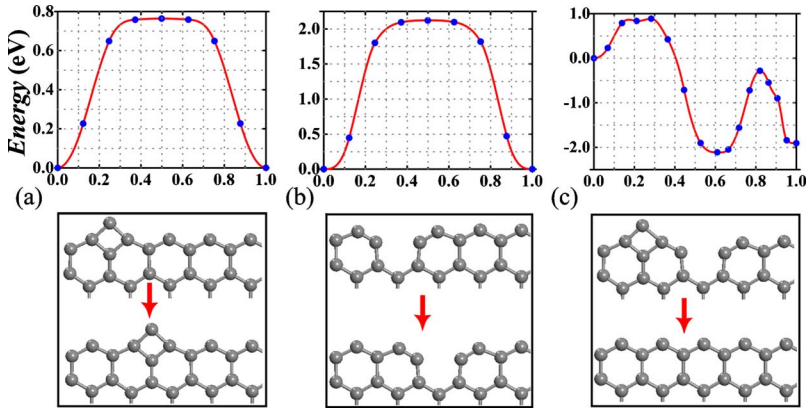
FIG. 1. (Color online) The MEP for (a) the carbon adatom migration, (b) the vacancy migration, and (c) the recombination of AVP located at one edge of the 7-ZGNR. The x axis is the reaction coordinate in each case. The corresponding initial and final structures are shown in the lower panel.

the interaction between defects, we use a supercell including eight unit cells of the ZGNR with the length along the ribbon axis of about 17.95 Å. In the transport calculations, considering that every defect has the same possibility of being located at the two edges in experiments, we choose ZGNRs with both edges having one defect as the models.

III. RESULTS AND DISCUSSION

We start by investigating the stable structures of adatom and vacancy defects at the edge of ZGNRs. As a result of the sp^2 hybridization in a graphene sheet, each edge atom of a perfect ZGNR has one dangling sp^2 orbital. When a carbon adatom is located at the ZGNR edge, it prefers to stay at the bridge site between two adjacent edge atoms to form two σ bonds [the lower panel of Fig. 1(a)]. However, when a vacancy is created at the edge site of the ZGNR by removing an edge carbon atom, the two carbon atoms adjacent to the vacancy, each having one dangling sp^2 bond, move away a little along opposite directions and form stronger bonds with their adjacent edge atoms [the lower panel of Fig. 1(b)]. And the bond length decreases from 1.38 to 1.25 Å. We further calculate the MEP for the migration of adatom and vacancy defects along the edge of the 7-ZGNR (with seven zigzag chains). The migration barrier (E_B) obtained for the edge adatom is 0.76 eV [the upper panel of Fig. 1(a)]. Although σ-bond breaking and rebonding are involved in this process, the free space in the edge area allows for an easy relaxation of neighboring atoms and substantially lowers the barrier. This barrier is only 0.30 eV higher than the diffusion barrier of a carbon adatom moving over a graphene surface.[25] On the other band, the calculated migration barrier of the vacancy is about 2.12 eV [the upper part of Fig. 1(b)], over three times of the barrier of carbon adatom, suggesting that the edge vacancy is much less mobile than the adatom.

In a thermodynamic sense, the rate coefficient k for the migration of edge defects is expressed as $\nu_G \exp(-E_B/k_B T)$, where the attempt frequency $\nu_G = \prod_{i=1}^{3N} \nu_i^{IS}/\prod_{i=1}^{3N-1} \nu_i^{TS}$ can be calculated using the van't Hoff-Arrhenius law within the harmonic approximation.[26,27] Herein ν_i^{IS} and ν_i^{TS} are, respectively, the normal-mode frequencies at the initial and transition states, and can be obtained from the phonon frequency calculation at each configuration. The calculated attempt frequency, ν_G, of the vacancy migration ($\sim 7 \times 10^{13}$ s^{-1}) is

higher than that of the carbon adatom ($\sim 3 \times 10^{13}$ s^{-1}). This is because the bonding between the edge atom and its adjacent atoms is stronger than that between the adatom and its adjacent atoms, leading to a higher vibrational frequency ν_i^{IS}. (Note: the migration of the vacancy can be viewed as the migration of the carbon edge atom.) The calculated rate coefficient of the adatom migration ($k \sim 5$ s^{-1}) is much larger than that of the vacancy migration ($k \sim 2 \times 10^{-22}$ s^{-1}) at room temperature ($T = 300$ K). This clearly demonstrates that the carbon adatom is quite mobile but the vacancy is almost immobile, consistent with the experimental observation that adatoms are generally much more mobile in the bulk or at the surface than vacancies.[28]

It should be noted that the edge adatoms and vacancies may recombine during their migration, which results in the formation of a stable edge structure. Without loss of generality, we consider the recombination process of the adatom-vacancy pair where an adatom and a vacancy are adjacent to each other. Figure 1(c) shows the MEP of the recombination, as well as the initial structure (AVP) and final structure (perfect edges). It can be seen that the 7-ZGNR with AVP is about 1.90 eV higher in energy than that with perfect edges. The MEP of the recombination is quite complicated, compared with those of migrations of the adatom and vacancy. Interestingly, it is found from the MEP that there exists a structure more stable (about 0.21 eV lower in energy) than the 7-ZGNR with perfect edges. Figure 2(a) shows the detailed structure corresponding to the minimum total energy in the MEP, with one R57 defect at the edge. This result is somewhat unexpected since for perfect carbon nanotubes (CNTs) or graphene, the introduction of the Stone-Wales defect (two pairs of R57) will always increase the total energy of CNTs or graphene.[29,30] Two very recent works have predicted that graphene could have periodic R57 edge structure,[16,17] which supports our result to some extent. However, the difference is that the R57 found here is not periodic and is formed from the recombination of the adatom and vacancy. Note that edge adatoms and vacancies can occur with high probability when ZGNRs are prepared in experiments. Thus, in the case of no hydrogenation of edges, local R57 structures are very likely to appear in practice as the adatoms migrate along the edge and the recombination of the adatom and vacancy proceeds.

As shown in Fig. 1(c), the energy barrier of the recombination (i.e., from the AVP to R57 edge structure) is about
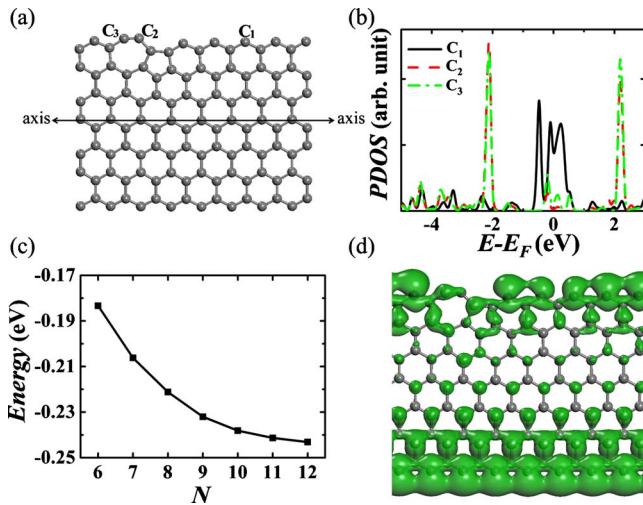
FIG. 2. (Color online) (a) The R57 which exists at one edge of the 7-ZGNR. (b) The PDOS of three edge carbon atoms [C_1, C_2, and C_3, as indicated in (a)]. (c) Calculated energy difference between the N-ZGNRs with one edge R57 defect and that with perfect edges as a function of the ribbon width (i.e., index N). (d) The isosurface of charge density (0.01 $e/Å^3$) within a 0.25 eV energy window (from −0.125 to 0.125 eV relative to Fermi energy) in the 7-ZGNR with one edge R57 defect.

0.89 eV.[31] The calculated rate coefficient k is ~ 0.1 s^{-1} at room temperature, fast enough to be observed in experimental time scale. Importantly, our further calculations indicate that the barrier and the rate coefficient are insensitive to the widths of ZGNRs. It is thus highly possible to form a R57 structure from the AVP at the edges of ZGNRs. In fact, two very recent experiments have already demonstrated that the migration or vaporization of carbon edge atoms plays an important role of edge reconstruction of graphene and GNRs.[32,33] Especially, the pentagon-heptagon ring can be clearly identified at the zigzag edge in transmission electron microscope images of graphene [see the supporting materials of Ref. 33 and Fig. 1 of Ref. 34], which supports our theoretical prediction of the stable R57 edge defect. On the other hand, we should note that although the perfect zigzag edge is less stable than the R57 edge structure in energy, the energy barrier of the transformation from the perfect zigzag edge to the R57 structure is quite high [~ 1.61 eV as shown in Fig. 1(c)], and the corresponding rate coefficient is small ($k \sim 1 \times 10^{-13}$ s^{-1} at room temperature). This means that once the perfect zigzag edges are formed, they are relatively stable and will not transform to the R57 edge structure at room temperature for a long time. Such a feature is just consistent with the recent microscopy observations of the perfect zigzag edges appearing under special experimental conditions.[32,33]

The high stability of the R57 edge, superior to the perfect edge, can be well understood by the formation of new bonds between edge atoms. Compared with 7-ZGNR with perfect edges, two edge atoms in the R57 structure [i.e., C_2 and C_3 in Fig. 2(a)] can form an additional bond since both of them have the dangling sp^2 orbitals. This can be clearly seen from two sharp peaks (representing bonding and antibonding states, respectively) in the projected density of states (PDOS)
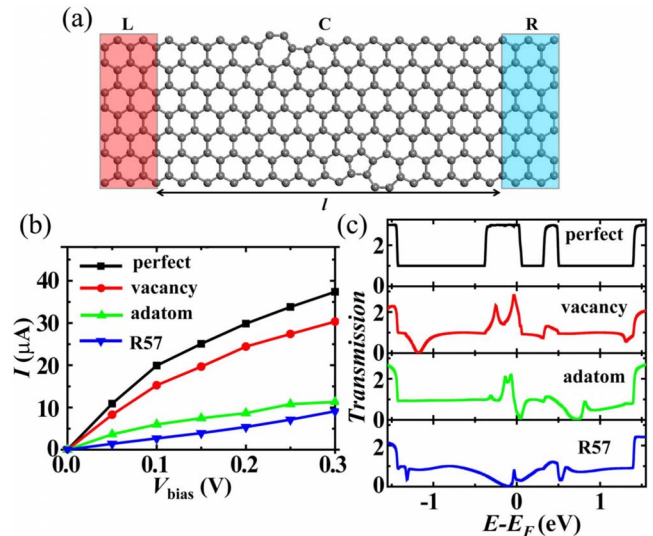

FIG. 3. (Color online) (a) Schematic structure of a two-probe 7-ZGNR system, where edge defects exist at the both edges. A bias voltage V_{bias} is applied to the central region with the length (l) of 14 unit cells. (b) I-V_{bias} curves and (c) transmission spectra under V_{bias}=0.1 V for 7-ZGNRs with perfect or defective edges.

of such two atoms [Fig. 2(b)]. The calculated C_2—C_3 bond length is about 1.23 Å, typical for —C≡C— triple bond, which is consistent with the result of the periodic R57 structure.[16,17] Therefore, the decrease in energy of the R57 edge structure reflects a compromise between the decrease in the total energy as a result of the formation of new bonds and the increase in energy due to the structural deformation of R57. In addition, our calculations show that the R57 structure can also exist at the open end of zigzag CNTs. For example, the total energy of open-ended (10,0) zigzag CNT with one R57 edge structure is 0.15 eV lower than that with perfect edge structure. Moreover, the energy difference between the ZGNRs with one R57 edge structure and with perfect edges monotonously decreases with the ribbon width [as shown in Fig. 2(c)]: the wider the ZGNR is, the more stable the R57 edge structure is.[35] This is because the stress induced by structural deformation can be released more easily as the width of ZGNRs increases. Typically, the energy difference is about −0.24 eV per R57 defect for the 12-ZGNR (about 2.4 nm wide).

For ZGNRs with perfect edges, two partially flat bands around the Fermi level, which come from π/π^* electrons and are mostly localized at the two edges for large wave vector (i.e., edge states), are responsible for the electron transmission under low bias voltages (V_{bias}).[12] The presence of edge defects will change the π/π^* state and profoundly influence the conduction mechanism.[36] To understand the role of edge defects in the transport behaviors of ZGNRs under bias voltages, we carry out extensive first-principles calculations of I-V_{bias} curves by using a two-probe system [Fig. 3(a)], where left (L) and right (R) leads are semi-infinite ZGNRs, and the central region (C) is a 7-ZGNR of 14 unit cell length with two edge defects (one at each edge). As shown in Fig. 3(b), the current (I) of the ZGNR with perfect edges increases rapidly as bias voltage increases, be-
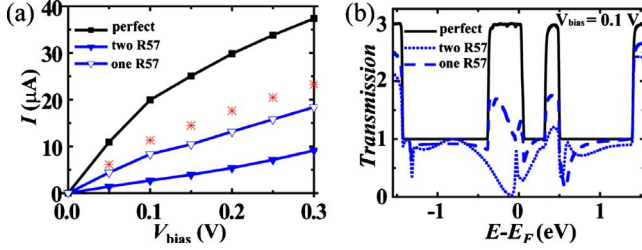
FIG. 4. (Color online) (a) I-V_{bias} curves and (b) transmission spectra under V_{bias}=0.1 V for 7-ZNGRs with perfect edges and with two R57 defective edges, and 7-ZGNR with one R57 defective edge and one perfect edge. The red stars in (a) indicate the average current of 7-ZGNRs with perfect edges and with two R57 defective edges under the same bias voltage.

cause there are at least one conductance quantum G_0 (arising from the π/π^* state) around the Fermi level (extra $2G_0$ arises from dangling bond states of edge atoms) [Fig. 3(c)]. The presence of any one kind of edge defects, however, always leads to a decrease in the current. For example, for V_{bias}=0.1 V, the currents of 7-ZGNRs with vacancy, adatom and R57 edge defects are 15.26 μA, 5.98 μA and 2.69 μA, respectively, which are all smaller than the current of 19.93 μA for the 7-ZGNR with perfect edges. More importantly, the current of the ribbon with the R57 defects drops drastically and the system even deviates from original metallic transport behavior of ZGNRs. This can be understood from the transmission spectrum (i.e., quantum conductance) of the 7-ZGNR under a certain bias voltage. As shown in Fig. 3(c), the transmission around the Fermi level for the R57 edge defect is much smaller than that for other cases. As mentioned before, the transport behavior of ZGNRs under low bias voltages is determined by the π/π^* state related to the edge states. Among three kinds of edge defects we discuss here, R57 edge defect destroys original hexagonal structure along the edges most seriously, and thus changes the original property of the π/π^* state notably [as shown in Fig. 2(d)], and causes a remarkable conductance suppression around the Fermi level.

We also calculate the I-V_{bias} curve and transmission spectrum for the 7-ZGNR containing only one R57 defect. The results are shown in comparison with those for the ribbons with two perfect edges and with two defective edges in Fig. 4. Under low bias voltages, the current of 7-ZGNR with one R57 edge defect is between those of 7-ZGNR with perfect edges and 7-ZGNR with two R57 defects at both edges, but a little less than their average value. This indicates that the R57 edge defect can significantly reduce the conductance along the defective edge but the conduction channel along the perfect edge without R57 defect is less affected even for narrow ribbons. The conduction characteristic can be understood from the transmission spectra (i.e., quantum conductance) of the 7-ZGNRs with three kinds of edges mentioned above. Under the same bias voltage, the conductance around the Fermi level of 7-ZGNR with one R57 edge defect is

smaller than that with perfect edges, but larger than that with two R57 defective edges. These results further verify the validity of our conclusion that the conductance is drastically suppressed by R57 edge defects in ZGNRs. Moreover, similar transport behaviors are also observed for 11-ZGNRs and fully H-passivated 7-ZGNRs with different defective edges (data not shown). These results confirm a drastic conductance suppression by R57 edge defects in ZGNRs.

Recent experiments showed that all narrow GNRs (from sub-10 nm to several tens of nanometer) by lithographical fabrication or chemical growth are semiconductors without evident crystallographic directional dependence[3,4,6] while numerous theoretical works predicted all perfect ZGNRs are metallic.[14] This implies a crucial role of the detailed edge structure in the transport properties of GNRs. In fact, under current experimental techniques, it is still very difficult to obtain GNRs with atomically smooth edges. Thus, our transport calculations based on the used model cannot lead to a direct comparison with present experimental measurements of GNRs, where the edge disorder is generally believed to play a key role in the transport characteristic of GNRs. Considering its high stability, however, we expect that the R57 edge defect may also be an important factor to determine the practical transport behavior of fabricated GNRs. Further studies on other kinds of edge defects as well as edge defect complexes are still needed to fully understand the overall effect of edge defects on the transport properties of GNRs.

IV. CONCLUSIONS

In summary, we have presented a detailed study on the migration of edge defects (adatom and vacancy) and the recombination of atom-vacancy pair in ZGNRs. The migration barriers of adatom and vacancy are 0.76 eV and 2.12 eV, respectively. The recombination process of the adatom-vacancy pair through the adatom migration, which could occur at room temperature by overcoming an activation barrier of 0.89 eV, will produce a more stable R57 edge structure. It indicates that the ideal ZGNR is less stable than the formed edge-defect structure. The current of ZGNRs with R57 edge defects drops drastically as a result of the notable suppression of conductance around the Fermi level. Our results, indicating a possible stable edge defect structure in experimentally fabricated ZGNRs, provide an explicit mechanism (in addition to the edge disorder) to understand why all narrow GNRs prepared in experiments are semiconductors.

*Present address: Fritz-Haber-Institut der Max-Planck-Gesellschaft, Faradayweg 4-6, 14195 Berlin, Germany.

†Present address: Department of Physics, University of Illinois at Urbana-Champaign, Urbana, Illinois 61801-3080, USA.

‡Corresponding author; dwh@phys.tsinghua.edu.cn

[1] M. I. Katsnelson, Mater. Today **10**, 20 (2007); A. K. Geim and K. S. Novoselov, Nature Mater. **6**, 183 (2007); A. H. Castro Neto, F. Guinea, N. M. R. Peres, K. S. Novoselov, and A. K. Geim, Rev. Mod. Phys. **81**, 109 (2009), and references therein.

[2] Z. Chen, Y. Lin, M. J. Rooks, and P. Avouris, Physica E **40**, 228 (2007).

[3] M. Y. Han, B. Ozyilmaz, Y. Zhang, and P. Kim, Phys. Rev. Lett. **98**, 206805 (2007).

[4] X. Li, X. Wang, L. Zhang, S. Lee, and H. Dai, Science **319**, 1229 (2008); X. Wang, Y. Ouyang, X. Li, H. Wang, J. Guo, and H. Dai, Phys. Rev. Lett. **100**, 206803 (2008).

[5] S. S. Datta, D. R. Strachan, S. M. Khamis, and A. T. Charlie Johnson, Nano Lett. **8**, 1912 (2008).

[6] L. Tapasztó, G. Dobrik, P. Lambin, and L. P. Biró, Nat. Nanotechnol. **3**, 397 (2008).

[7] L. Weng, L. Zhang, Y. P. Chen, and L. P. Rokhinson, Appl. Phys. Lett. **93**, 093107 (2008).

[8] Y.-W. Son, M. L. Cohen, and S. G. Louie, Nature (London) **444**, 347 (2006); Phys. Rev. Lett. **97**, 216803 (2006).

[9] V. Barone, O. Hod, and G. E. Scuseria, Nano Lett. **6**, 2748 (2006).

[10] Q. Yan, B. Huang, J. Yu, F. Zheng, J. Zang, J. Wu, B.-L. Gu, F. Liu, and W. H. Duan, Nano Lett. **7**, 1469 (2007); B. Huang, F. Liu, J. Wu, B.-L. Gu, and W. H. Duan, Phys. Rev. B **77**, 153411 (2008).

[11] A. Rycerz, J. Tworzydło, and C. W. J. Beenakker, Nat. Phys. **3**, 172 (2007).

[12] Z. Li, H. Y. Qian, J. Wu, B.-L. Gu, and W. H. Duan, Phys. Rev. Lett. **100**, 206802 (2008).

[13] K. A. Ritter and J. W. Lyding, Nature Mater. **8**, 235 (2009).

[14] K. Nakada, M. Fujita, G. Dresselhaus, and M. S. Dresselhaus, Phys. Rev. B **54**, 17954 (1996); Y. Miyamoto, K. Nakada, and M. Fujita, *ibid.* **59**, 9858 (1999).

[15] Y. Yoon and J. Guo, Appl. Phys. Lett. **91**, 073103 (2007); D. Basu, M. J. Gilbert, L. F. Register, S. K. Banerjee, and A. H. MacDonald, *ibid.* **92**, 042114 (2008); D. Gunlycke, D. A. Areshkin, and C. T. White, *ibid.* **90**, 142104 (2007); A. Lherbier, B. Biel, Y.-M. Niquet, and S. Roche, Phys. Rev. Lett. **100**, 036803 (2008); T. C. Li and S.-P. Lu, Phys. Rev. B **77**, 085408 (2008); M. Evaldsson, I. V. Zozoulenko, H. Xu, and T. Heinzel, *ibid.* **78**, 161407(R) (2008); B. Huang, M. Liu, N. Su, J. Wu, W. H. Duan, B. L. Gu, and F. Liu, Phys. Rev. Lett. **102**, 166404 (2009); E. R. Mucciolo, A. H. Castro Neto, and C. H. Lewenkopf, Phys. Rev. B **79**, 075407 (2009).

[16] T. Wassmann, A. P. Seitsonen, A. M. Saitta, M. Lazzeri, and F. Mauri, Phys. Rev. Lett. **101**, 096402 (2008).

[17] P. Koskinen, S. Malola, and H. Häkkinen, Phys. Rev. Lett. **101**, 115502 (2008).

[18] G. Kresse and J. Furthmüller, Phys. Rev. B **54**, 11169 (1996).

[19] G. Kresse and D. Joubert, Phys. Rev. B **59**, 1758 (1999).

[20] J. P. Perdew, K. Burke, and M. Ernzerhof, Phys. Rev. Lett. **77**, 3865 (1996).

[21] G. Henkelman, B. P. Uberuaga, and H. Jónsson, J. Chem. Phys. **113**, 9901 (2000).

[22] M. Brandbyge, J. L. Mozos, P. Ordejón, J. Taylor, and K. Stokbro, Phys. Rev. B **65**, 165401 (2002).

[23] It should be noted that using electronic structures calculated with density-functional theory for transport calculations might lead to unreliable results for some systems, F. Evers and K. Burke, in *Nano and Molecular Electronics Handbook*, edited by S. E. Lyshevski (CRC Press, Cleveland/Boca Raton, 2007), p. 24-1. For example, this mean fieldlike, one-electron approach is not able to describe pronounced many-body effects which may appear in some transport processes.

[24] G. Stefanucci and C.-O. Almbladh, Phys. Rev. B **69**, 195318 (2004); G. Stefanucci, S. Kurth, E. K. U. Gross, and A. Rubio, in *Molecular and Nano Electronics: Analysis, Design and Simulation*, Elsevier Series on Theoretical and Computational Chemistry Vol. 17, edited by J. Seminario (Elsevier, New York, 2007), p. 247.

[25] P. O. Lehtinen, A. S. Foster, A. Ayuela, A. Krasheninnikov, K. Nordlund, and R. M. Nieminen, Phys. Rev. Lett. **91**, 017202 (2003).

[26] G. H. Vineyard, J. Phys. Chem. Solids **3**, 121 (1957).

[27] H. Lee, J. Li, G. Zhou, W. H. Duan, G. Kim, and J. Ihm, Phys. Rev. B **77**, 235101 (2008).

[28] F. Banhart, Rep. Prog. Phys. **62**, 1181 (1999).

[29] L. G. Zhou and S. Shi, Appl. Phys. Lett. **83**, 1222 (2003).

[30] V. H. Crespi, M. L. Cohen, and A. Rubio, Phys. Rev. Lett. **79**, 2093 (1997).

[31] To check the validity of our model used, we do complementary energetics calculations for 7-ZGNR with two defective edges. The obtained recombination barrier of an AVP pair is almost the same as that of the 7-ZGNR with one perfect edge and the defect being located on the other edge.

[32] X. Jia, M. Hofmann, V. Meunier, B. G. Sumpter, J. Campos-Delgado, J. M. Romo-Herrera, H. Son, Y.-P. Hsieh, A. Reina, J. Kong, M. Terrones, and M. S. Dresselhaus, Science **323**, 1701 (2009).

[33] Ç. Ö. Girit, J. C. Meyer, R. Erni, M. D. Rossell, C. Kisielowski, L. Yang, C.-H. Park, M. F. Crommie, M. L. Cohen, S. G. Louie, and A. Zettl, Science **323**, 1705 (2009).

[34] P. Koskinen, S. Malola, and H. Häkkinen, Phys. Rev. B **80**, 073401 (2009).

[35] Comparative calculations using local-density approximation of the Ceperley-Alder form [D. M. Ceperley and B. J. Alder, Phys. Rev. Lett. **45**, 566 (1980)] show similar monotonous decrease in the energy difference with increasing ribbon width.

[36] T. B. Martins, R. H. Miwa, A. J. R. da Silva, and A. Fazzio, Phys. Rev. Lett. **98**, 196803 (2007).